Thermal background blurring on ADONIS system

H. Geoffray[1]

[1] Laboratoire d'Astrophysique, Observatoire de Grenoble,
Université Joseph Fourier, BP 53, F-38041, Grenoble Cedex 9

Abstract – We evidence a strong and inhomogeneous background emission in the 3-5 μm wavelength range on ESO ADONIS Adaptive Optics system equipped with the COMIC camera. In this poster, we show that the correction process blurs the image of the thermal background emission. Even with a chopping/nodding-like observing method, a residual still remains after substraction of the sky/instrumental thermal background emission. This effect has been characterized both temporally and spatially on the images. The resulting loss in performance is discussed.

1 Introduction

The characteristics of the ADONIS bench (Beuzit *et al.*, 1997) thermal background emission are the following:

- 95% (resp. 85%) of the thermal emission in L' band (resp. M band) is due to instrumental emission.
- 70% of the instrumental emission comes from the Adaptive Optics (AO) bench (Le Mignant *et al.*, 1998).
- The thermal background emission is highly inhomogeneous with a dispersion over the available imaging field corresponding to a flux of the order of 5000 electrons/s *rms* in L' band (see Figure 1)

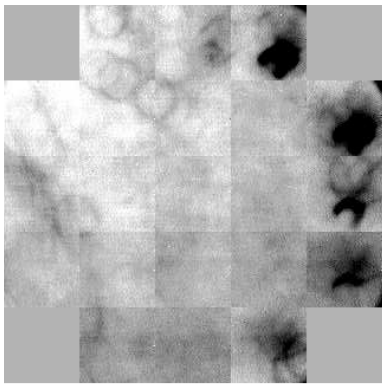

Figure 1: Thermal instrumental background emission on the available ADONIS field. Cuts are set to +/- 2σ around the image mean value.

A chopping procedure is currently applied on the ADONIS system by means of an ON/OFF mirror. This chopping procedure aims at removing the sky background emission from the images. However, the sky substracted images exhibit strong background inhomogeneities. In the following, the sky substracted image will be noted (ON-OFF). In order to substract instrumental background emission, a nodding-like procedure has to be used. This nodding-like method consists in offsetting the telescope and re-perform the same chopping procedure as previously done.

In section 2, we show the limitations of this procedure as the AO system actually modulates the instrumental thermal background emission. In section 3, this effect is characterized both spatially and temporally. A simulation is presented in section 4, whose primary goal is to clarify the origin of this effect. In this framework, the imaging performances are discussed in section 5. A conclusion is given in section 6.

2 Thermal background "blurring"

2.1 Open-loop chopping

In this case, the telescope has been moved to an empty sky position where the chopping procedure has been repeated. Therefore, the AO system is inactive on the empty sky position. The empty-field (ON-OFF) image has been substracted to the on-object (ON-OFF) image and gives the result displayed on figure 2 (M band). A strong residual pattern remains on this image. Its value corresponds to a flux of the order of 1000 electrons/s *rms* in L' band and 4000 electrons/s in M band.

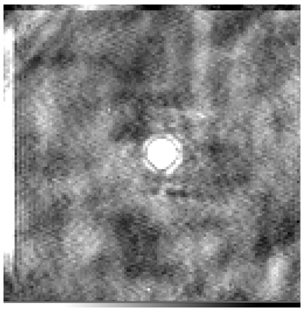

Figure 2: Reduced image obtained with open-loop chopping+nodding-like procedure.

2.2 Closed-loop chopping

In that case, the AO system is active during the instrumental thermal emission recording. The image displayed here (figure 3) shows the substraction of 2 (ON-OFF) images taken on the same object and gives an estimate of the residual pattern. It has been reduced to lower values: it is of the order of 200 electrons/s *rms* in L' band and 1000 electrons/s *rms* in M band. This procedure gives better results, but can be only applied on ADONIS when the scientific object is not used as wavefront sensor reference.

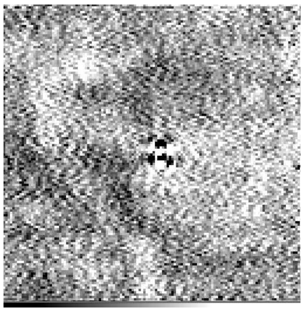

Figure 3: Test image obtained with closed-loop chopping+nodding-like procedure.

3 Noise Characterization

We performed statistics on image cubes in order to study the spatial and temporal variation from one image plane to the other.

3.1 Spatial noise

Figure 4 and 5 show the integrated count variation between 2 empty zones of the image. Each point represents a plane of the cube. Figure 4 corresponds to a cube taken with the AO system working while figure 5 corresponds to a cube taken with the AO system not working. The shift between the two loci is attributed to instrumental emission variations between the ON and OFF positions. A strong dispersion is clearly seen when AO system is active, which results in a spatial noise on the average image.

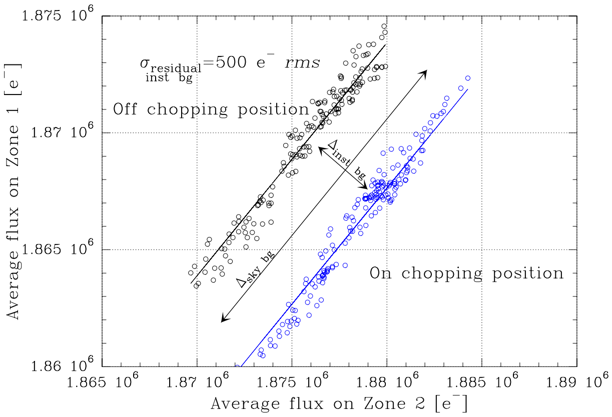

Figure 4: Average flux on zone 1 of the image vs average flux on zone 2 of the image, AO "on". Linear fits have been performed for the ON and OFF positions.

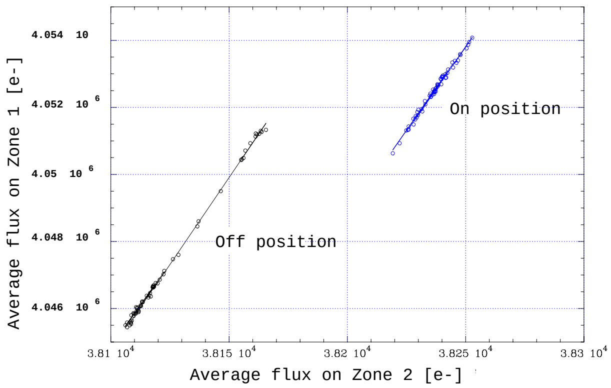

Figure 5: Average flux on zone 1 of the image vs average flux on zone 2 of the image, AO "off".

3.2 Temporal noise

Figure 6 gives the variance image of a cube. It corresponds to the pixel to pixel temporal noise since each image of the cube has been substracted from its mean value to remove correlated background emission variations on the field. The large scale pattern of this variance image is reproducible from one cube to the other. Figure 7 displays the average variance on the image as a function of the background level. Each point corresponds to an image cube, taken under various conditions (background level, airmass, integration time). Empty symbols correspond to cubes taken with AO system "off" and filled symbols correspond to the same sequence with AO system "on". From figure 7, we can evaluate the noise budget due to the correction process:

- 500 electrons/s *rms* in L' band.
- 1500 electrons/s *rms* in M band.

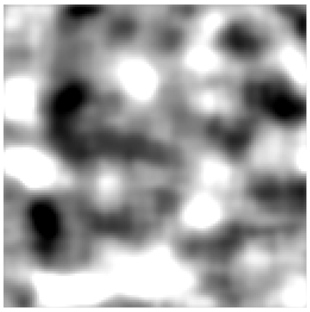

Figure 6: Temporal variance image of an image cube.

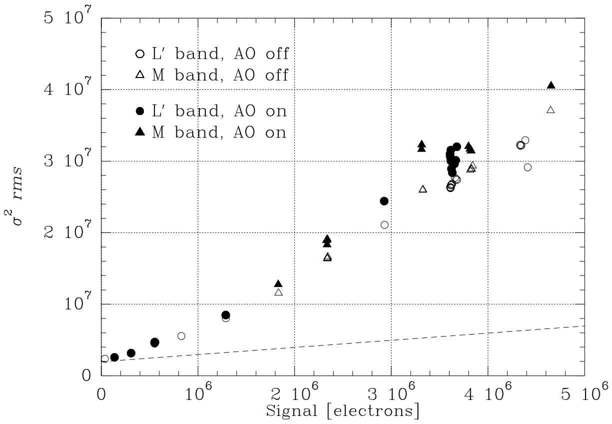

Figure 7: Average temporal variance over the image vs background level.

4 Simulation

The noise sources previously discussed are induced by the AO system. The goal of the simulation is to model these noise sources. The basic assumption is to attribute them to the first order correction, namely tip-tilt correction, since the tip-tilt mirror is not located in a pupil conjugate plane.

Therefore, the fundamentals of this simulation are:

- the tip-tilt correction counteracts image motion. Consequently, we need to know the statistics of the image motion.
- the main source of background inhomogeneities is located before the tip-tilt mirror, namely on ADONIS M1 mirror.

The deviation α' of the image from its average position has a Gaussian probability density (Roddier, 1981):

$$\mathcal{P}(\alpha\prime) = \frac{1}{\pi\sigma_m^2}\exp(-\frac{|\alpha'|^2}{\sigma_m^2})$$

with standard deviation given by:

$$\sigma_m^2 \simeq 0.36(\frac{\lambda}{D})^{\frac{1}{3}}(\frac{\lambda}{r_0})^{\frac{5}{3}}$$

Thus, the long exposure image of the background (the "blurred" image of the thermal background emission) is:

$$I_{mean}(\alpha) = \int \mathcal{P}(\alpha\prime) I_{static}(\alpha - \alpha\prime) d\alpha\prime$$

and the sigma image is given by:

$$\sigma(\alpha)^2 = \mathcal{P}(\alpha) * I_{static}(\alpha)^2 - (\mathcal{P}(\alpha) * I_{static}(\alpha))^2$$

Where I_{static} is the static image of the thermal background emission (see figure 1). As a result:

- the long exposure image of the thermal background emission provides an evaluation of the spatial noise.
- the variance image of the thermal background emission provides an evaluation of the temporal noise.

The static image of the thermal background (cf figure 1) has been convolved with a gaussian of FWHM 0.25" ($r_0 \simeq 15cm$). The simulation is in good agreement with the observed dispersions (see section 2.1): it gives a spatial noise of 700 electrons/s rms and an average variance on the image of 400 electrons/s *rms* in L' band (see figure 8).

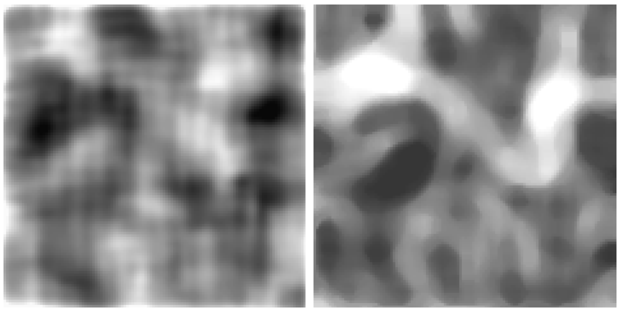

Figure 8: Simulation of the spatial dispersions image (left) and of the temporal variance image (right) induced by AO; these images can be compared to figure 2 and 6 respectively.

5 Performances

The spatial noise strongly affects the noise equivalent magnitude (NEM) (see Figure 9). The performance loss has been calculated for the COMIC camera (Lacombe *et al.*, 1998):

- Open-loop chopping (AO off) gives a performance loss of 3 mag. in L' and 4 mag. in M for an integration time of 1000s, compared to the thermal background limited noise.
- Closed-loop chopping (AO on) gives a performance loss of 1.4 mag. in L' band and 2 mag. in M band for an integration time of 1000s, compared to the thermal background limited noise.

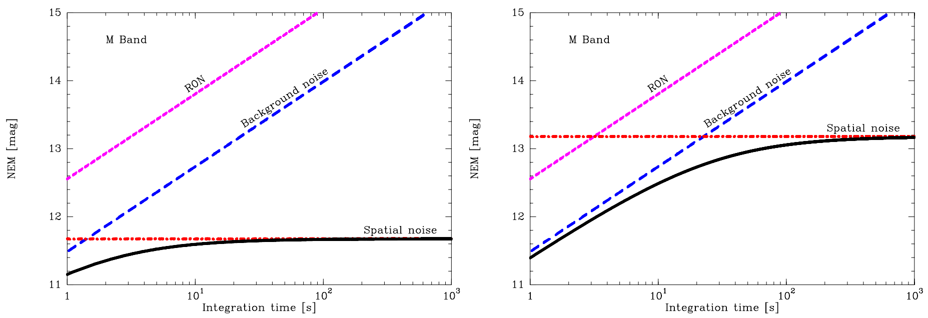

Figure 9: NEM vs integration time in the case of open-loop chopping (left) and in the case of closed-loop chopping (right).

6 Conclusion

In this paper, we showed that thermal background emission is modulated by the AO system. This effect has been attributed to tip-tilt correction.
For further AO instrument design, the following requirements should be met:

- better homogeneities of the thermal background emission is necessary,
- closed-loop chopping appears to be necessary. This can be achieved by using a counter chopping system.

References

Beuzit, J.-L., Demailly, L., Gendron, E., Gigan, P. *et al.* 1997, Adaptive Optics on a 3.6-Meter Telescope. The ADONIS System., *Experimental Astronomy* **7**, 285.

Lacombe, F., Marco, O., Geoffray, H., Beuzit, J.-L. *et al.* 1998, Adaptive Optics Imaging at 1-5 Microns on Large Telescopes:The COMIC Camera for ADONIS, *Public. of the Astron. Soc. Pac.* **110**, 1087.

Le Mignant, D., Gendron, E. & Marchis, F. 1998, The ESO ADONIS AO system: Study of the 3-5 μm background emissivity., *ESO/OSA Topical meeting on Astronomy with Adaptive Optics,* this volume.

Roddier, F. 1981, *The effect of atmospherical turbulence in optical astronomy*, Progress in optics, XIX, North-Holland Publishing Co. (Amsterdam), E. Wolf ed.